



Hyperactivity of the transcription factor Nrf2 causes metabolic reprogramming in mouse esophagus

Received for publication, September 22, 2018, and in revised form, November 3, 2018. Published, Papers in Press, November 8, 2018, DOI 10.1074/jbc.RA118.005963

Junsheng Fu^{†S1}, Zhaohui Xiong^{S1}, Caizhi Huang^S, Jing Li[¶], Wenjun Yang^{||}, Yuning Han[¶], Chorlada Paiboonrungruan^S, Michael B. Major^{**}, Ke-Neng Chen^{††}, Xiaozheng Kang^{††2}, and Xiaoxin Chen^{S S S 3}

From the [†]College of Life Sciences, Fujian Agriculture and Forestry University, Fuzhou, Fujian Province 350002, China, the ^SCancer Research Program, Julius L. Chambers Biomedical Biotechnology Research Institute, North Carolina Central University, Durham, North Carolina 27707, the [¶]Department of Thoracic Surgery, Ningxia Medical University General Hospital, Yinchuan, Ningxia 750004, China, the ^{||}Key Laboratory of Fertility Preservation and Maintenance (Ministry of Education), Cancer Institute of the General Hospital, Ningxia Medical University, Yinchuan, Ningxia 750004, China, the ^{**}Department of Cell Biology and Physiology, University of North Carolina, Chapel Hill, North Carolina 27599, the ^{††}Key Laboratory of Carcinogenesis and Translational Research (Ministry of Education), The First Department of Thoracic Surgery, Peking University Cancer Hospital and Institute, Beijing 100142, China, and the ^{S S S}Center for Esophageal Disease and Swallowing, Division of Gastroenterology and Hepatology, Department of Medicine, University of North Carolina, Chapel Hill, North Carolina 27599

Edited by Xiao-Fan Wang

Mutations in the genes encoding nuclear factor (erythroid-derived 2)-like 2 (NRF2), Kelch-like ECH-associated protein 1 (KEAP1), and cullin 3 (CUL3) are commonly observed in human esophageal squamous cell carcinoma (ESCC) and result in activation of the NRF2 signaling pathway. Moreover, hyperactivity of the transcription factor Nrf2 has been found to cause esophageal hyperproliferation and hyperkeratosis in mice. However, the underlying mechanism is unclear. In this study, we aimed to understand the molecular mechanisms of esophageal hyperproliferation in mice due to hyperactive Nrf2. Esophageal tissues were obtained from genetically modified mice that differed in the status of the *Nrf2* gene and genes in the same pathway (*Nrf2*^{-/-}, *Keap1*^{-/-}, *K5Cre;Pkm2*^{fl/fl}; *Keap1*^{-/-}, and WT) and analyzed for metabolomic profiles, Nrf2 ChIP-seq, and gene expression. We found that hyperactive Nrf2 causes metabolic reprogramming and up-regulation of metabolic genes in the mouse esophagus. One of the glycolysis genes encoding pyruvate kinase M2 (*Pkm2*) was not only differentially up-regulated, but also glycosylated and oligomerized, resulting in increased ATP biosynthesis. However, constitutive knockout of *Pkm2* failed to inhibit this esophageal phenotype *in vivo*, and this failure may have been due to compensation by *Pkm1* up-regulation. Transient inhibition of *NRF2* or glycolysis inhibited the growth of human ESCC cells in which *NRF2* is hyperactive *in vitro*. In

summary, hyperactive Nrf2 causes metabolic reprogramming in the mouse esophagus through its transcriptional regulation of metabolic genes. Blocking glycolysis transiently inhibits cell proliferation and may therefore have therapeutically beneficial effects on *NRF2*^{high} ESCC in humans.

Esophageal cancer affects 16,940 adults in the United States, and the 5-year survival rate is 18% (1). There are mainly two histological types of esophageal cancer, squamous cell carcinoma (ESCC)⁴ and adenocarcinoma, each having a distinct etiology. Low income, moderate/heavy alcohol intake, tobacco use, and infrequent consumption of raw fruits and vegetables account for almost all cases of ESCC (2). With the recent technological advances in NextGen sequencing, human ESCC samples from North and South America, China, Japan, Vietnam, and Malawi have been sequenced. Among many gene mutations, nuclear factor (erythroid-derived 2)-like 2 (NRF2 or NFE2L2) mutations are commonly seen with a frequency over 5%, even up to ~20% in certain reports. Mutations in other genes of the NRF2 signaling pathway, Kelch-like ECH associated protein 1 (KEAP1) and cullin 3 (CUL3), are relatively less common. *NRF2* mutations are mostly located in the DLG and ETGE motifs (KEAP1-binding domain) and the DNA-binding domain, whereas *KEAP1* mutations tend to be scattered across the whole gene. *NRF2* mutations and *KEAP1* mutations tend to be mutually exclusive (3, 4).

As a major cellular defense mechanism, the NRF2 signaling pathway is known to regulate expression of enzymes involved in detoxification and anti-oxidative stress response. NRF2 forms heterodimers with small MAF proteins and binds to the anti-oxidant-response elements of target genes when cells are

This work was supported by China Scholarship Council Grant 201608350016, National Institutes of Health Research Grants U54 AA019765, U54 CA156735, and U54 MD012392, and Beijing Municipal Administration of Hospitals Youth Program Grant QML20171106. The authors declare that they have no conflicts of interest with the contents of this article. The content is solely the responsibility of the authors and does not necessarily represent the official views of the National Institutes of Health.

This article contains Files S1–S7.

¹ Both authors contributed equally to this work.

² To whom correspondence may be addressed: Key Laboratory of Carcinogenesis and Translational Research (Ministry of Education), The First Department of Thoracic Surgery, Peking University Cancer Hospital and Institute, Beijing 100142, China. E-mail: kangxz@hsc.pku.edu.cn.

³ To whom correspondence may be addressed: Cancer Research Program, Julius L. Chambers Biomedical Biotechnology Research Institute, North Carolina Central University, 700 George St., Durham, NC 27707. Tel.: 919-530-6425; Fax: 919-530-7780; E-mail: lchen@ncu.edu.

This is an open access article under the CC BY license.

⁴ The abbreviations used are: ESCC, esophageal squamous cell carcinoma; G6PD, glucose-6-phosphate dehydrogenase; GSA, gene set analysis; HK, hexokinase; IHC, immunohistochemical staining; PCNA, proliferating cell nuclear antigen; PK, pyruvate kinase; Pkm, pyruvate kinase M; PPP, pentose phosphate pathway; SAM, significance analysis of microarrays; ANOVA, analysis of variance; 2DG, 2-deoxy-D-glucose; GAPDH, glyceraldehyde-3-phosphate dehydrogenase; ChIP-seq, ChIP-sequencing.

Hyperactive *Nrf2* in the esophagus

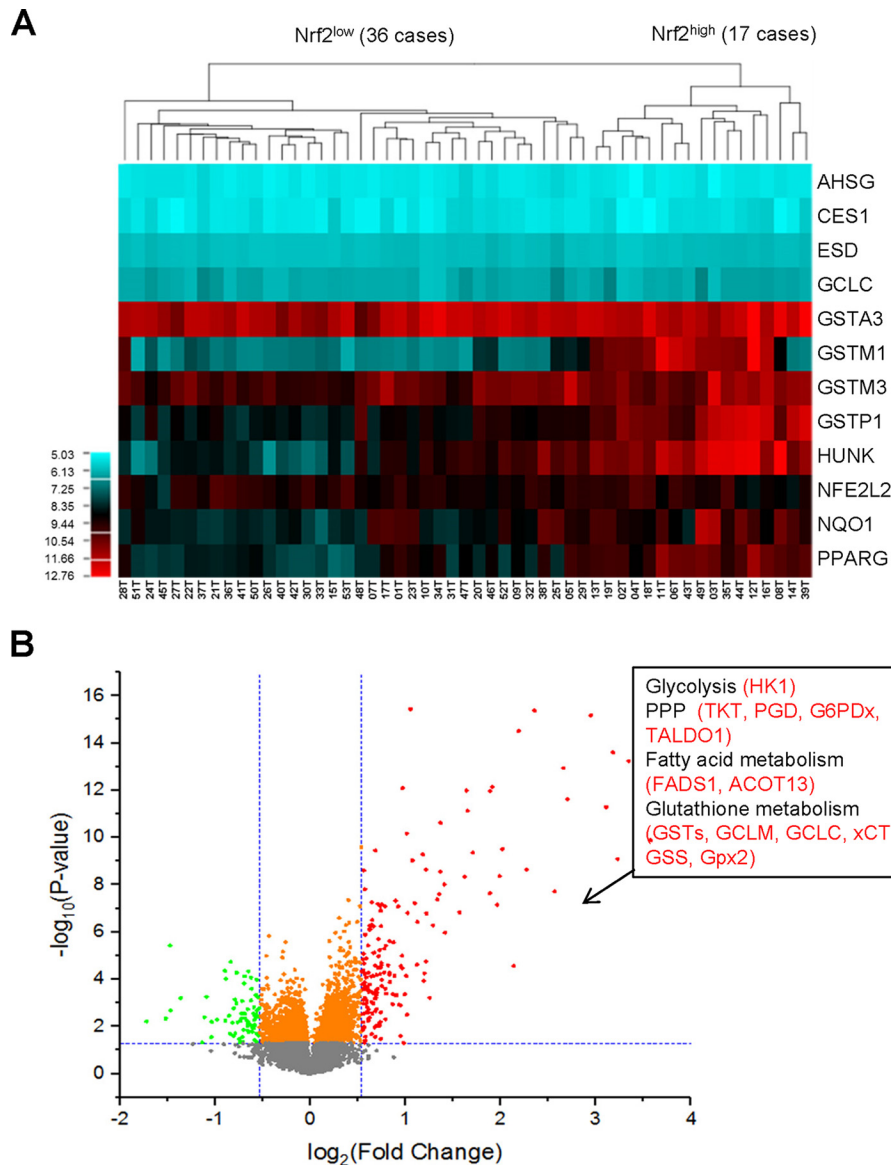


Figure 1. Hyperactive NRF2 was associated with up-regulation of metabolic genes. Fifty three cases of ESCC were clustered into two groups, NRF2^{high} ($n = 17$) and NRF2^{low} ($n = 36$), based on microarray data of esophagus-specific NRF2 target genes (GSE23400 dataset) (A). After two-class SAM analysis, the volcano graph showed that multiple metabolic genes were significantly up-regulated enriched in NRF2^{high} ESCC compared with NRF2^{low} ESCC (B).

exposed to oxidative stress or xenobiotics. KEAP1 inhibits the function of NRF2 by retaining NRF2 in the cytoplasm under normal physiological conditions and by allowing nuclear translocation of NRF2 under stress conditions (5). In fact, *NRF2* and *KEAP1* have been classified among 291 high-confidence cancer driver genes (6). NRF2 signaling pathway has long been recognized as a double-edged sword in carcinogenesis (7, 8). On the one hand, chemical or genetic activation of NRF2 induced cytoprotective enzymes and thus provided protection against chemical carcinogenesis in multiple models (9). *Nrf2*^{-/-} mice were more susceptible to chemical carcinogenesis than WT counterparts (10, 11). On the other hand, cancer cells can hijack the NRF2 signaling pathway for their survival through mechanisms that lead to constitutive activation of NRF2 signaling, such as somatic mutations of KEAP1/NRF2/CUL3, accumulation of disruptor proteins, skipping of *NRF2* exon 2, KEAP1 succinylation,

KEAP1 hypermethylation, increased NRF2 expression, and electrophilic attack by oncometabolites. As a consequence, NRF2 hyperactivation promoted cell proliferation, conferred radiochemoresistance to cancer cells, promoted metabolic reprogramming, and accelerated distant metastases (12–16). Therefore, NRF2 signaling has been regarded as a molecular target for cancer therapy (17).

The important role of the NRF2 signaling pathway in the esophagus was first revealed in a mouse study. Genetic activation of *Nrf2* in *Keap1*^{-/-} mice resulted in esophageal hyperproliferation and hyperkeratosis (18). To our best knowledge, all transcriptionally impacted genes downstream of *Keap1* knockout are *Nrf2*-responsive, although it is still possible that these KEAP1 substrates may still impact NRF2-independent transcription. Among the KEAP1 substrates other than NRF2 (19–26), WTX, PALB2, SQSTM1/P62, DPP3, and CDK20 proteins bind KEAP1 via an “ETGE” motif to displace NRF2, thus inhib-

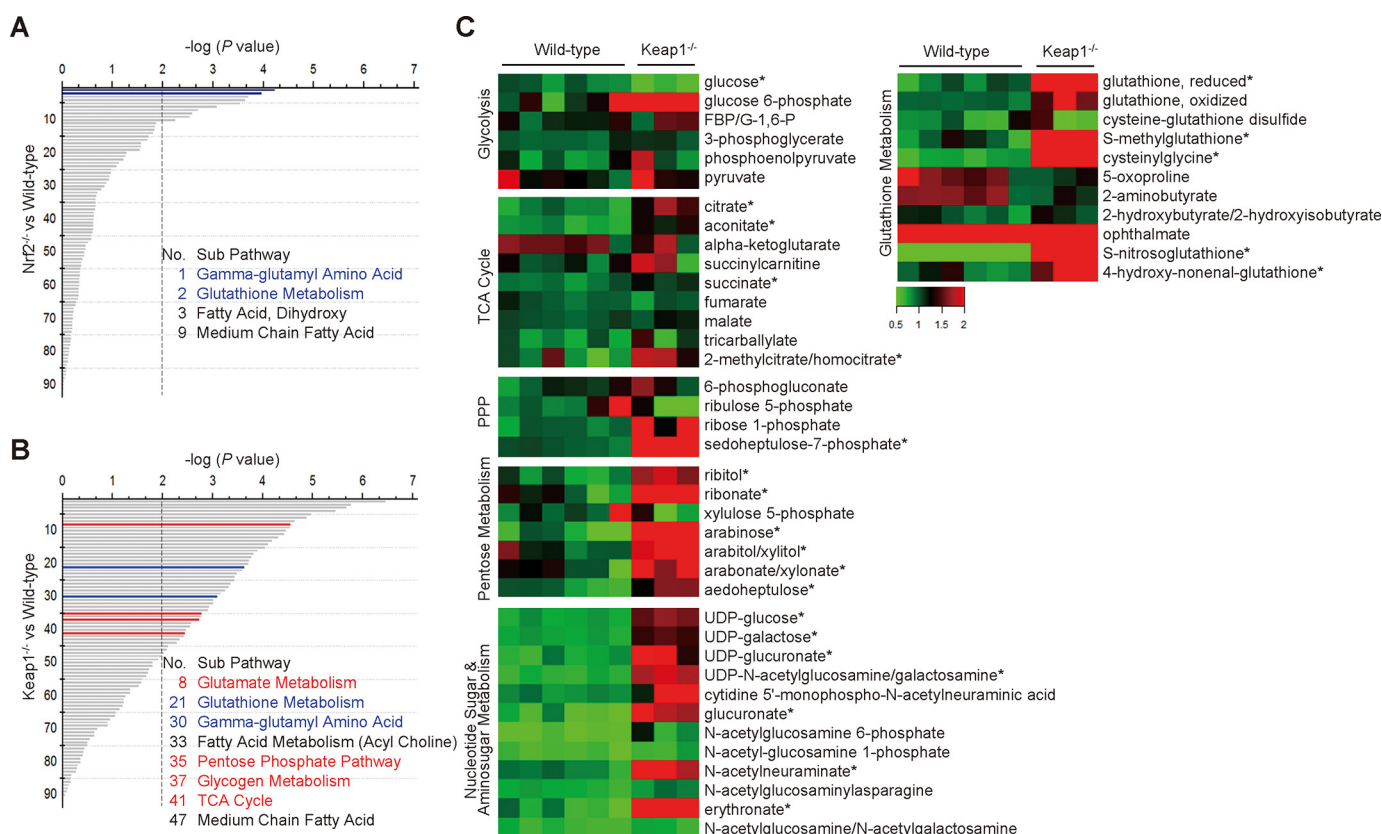


Figure 2. Hyperactive Nrf2 altered the metabolic profile in mouse esophagus. 833 metabolites on 93 subpathways were quantified and compared between $Nrf2^{-/-}$ esophagus ($n = 6$) and WT esophagus ($n = 6$) (A) and between $Keap1^{-/-}$ esophagus ($n = 3$) and WT esophagus. p values were determined using two-way ANOVA. B, subpathways each represented by a bar were regarded significantly different between two groups if $-\log(P)$ is higher than 2 (dashed line). Subpathways are ranked based on the value of $-\log(P)$. GSH metabolism subpathways (blue) and energy metabolism subpathways (red) are highlighted. Heatmaps showed changes of the metabolites on the subpathways of glycolysis, TCA cycle, PPP, pentose metabolism, nucleotide-sugar and amino-sugar metabolism, and GSH metabolism by comparing $Keap1^{-/-}$ esophagus with WT esophagus (C). *, $p < 0.05$. p values were determined using Student's t test.

iting NRF2 ubiquitination and driving NRF2-dependent transcription. In fact, $Keap1^{-/-}$ mice died within 3 weeks, and $Nrf2^{-/-};Keap1^{-/-}$ completely rescued the phenotype (18). $K5Cre;Nrf2^{fl/fl};Keap1^{-/-}$ mice did not develop any esophageal phenotype of $Keap1^{-/-}$ mice (27). We also found that $Nrf2$ target genes and gene sets associated with oxidoreductase activity, mitochondrial biogenesis, and energy metabolism were down-regulated in the $Nrf2^{-/-}$ esophagus. Consistent with these observations, ATP biogenesis and CoxIV (a mitochondrial marker) were also down-regulated (28). Previous ChIP-seq experiments have shown that NRF2 as a transcription factor regulates transcription of hundreds of genes in human lymphoblastoid cells (29), mouse macrophages (30), mouse embryonic fibroblasts (31), and mouse hepatoma cells (32).

Therefore, we hypothesized that hyperactive Nrf2 caused esophageal hyperproliferation and hyperkeratosis through transcriptional regulation of gene expression. Using genetically modified mice with various NRF2 status ($Nrf2^{-/-}$, WT, and $Keap1^{-/-}$), here we aimed to understand how hyperactive Nrf2 causes the esophageal phenotype in mice.

Results

Hyperactive NRF2 in human ESCC was associated with overexpression of metabolic genes

Using gene microarray data of 53 cases of human ESCC (33) (GEO23400), we performed clustering analysis with a list of

esophagus-specific NRF2 target genes (34), and we found two clusters, NRF2^{high} ($n = 17$) and NRF2^{low} ($n = 36$) (Fig. 1A). By comparing gene expression between these two groups, we found that a group of metabolic genes involved in glycolysis, pentose phosphate pathway (PPP), fatty acid metabolism, and GSH metabolism was overexpressed in NRF2^{high} ESCC (Fig. 1B; File S1). This observation suggested that NRF2 regulates the expression of metabolic genes in the esophagus.

Hyperactive Nrf2 resulted in metabolic reprogramming in mouse esophagus

833 metabolites on 93 subpathways were analyzed by a biochemical profiling platform. With $p < 0.01$ as the cutoff, 10 subpathways were significantly different between WT esophagus and $Nrf2^{-/-}$ esophagus (Fig. 2A), and 47 subpathways between WT esophagus and $Keap1^{-/-}$ esophagus (Fig. 2B). Among these subpathways, GSH metabolism and γ -glutamyl amino acid are known to be subject to Nrf2 regulation. Interestingly, multiple subpathways of carbohydrate metabolism and fatty acid metabolism were identified, for example, PPP, TCA cycle, and glycogen metabolism in the $Keap1^{-/-}$ esophagus (File S2 and S3). Heatmaps of glycolysis metabolites, TCA cycle metabolites, PPP metabolites, pentose metabolites, and nucleotide-sugar and amino-sugar metabolites showed an overall tendency of enhanced metabolism in $Keap1^{-/-}$ esophagus as compared with WT esophagus. Enhancement of GSH

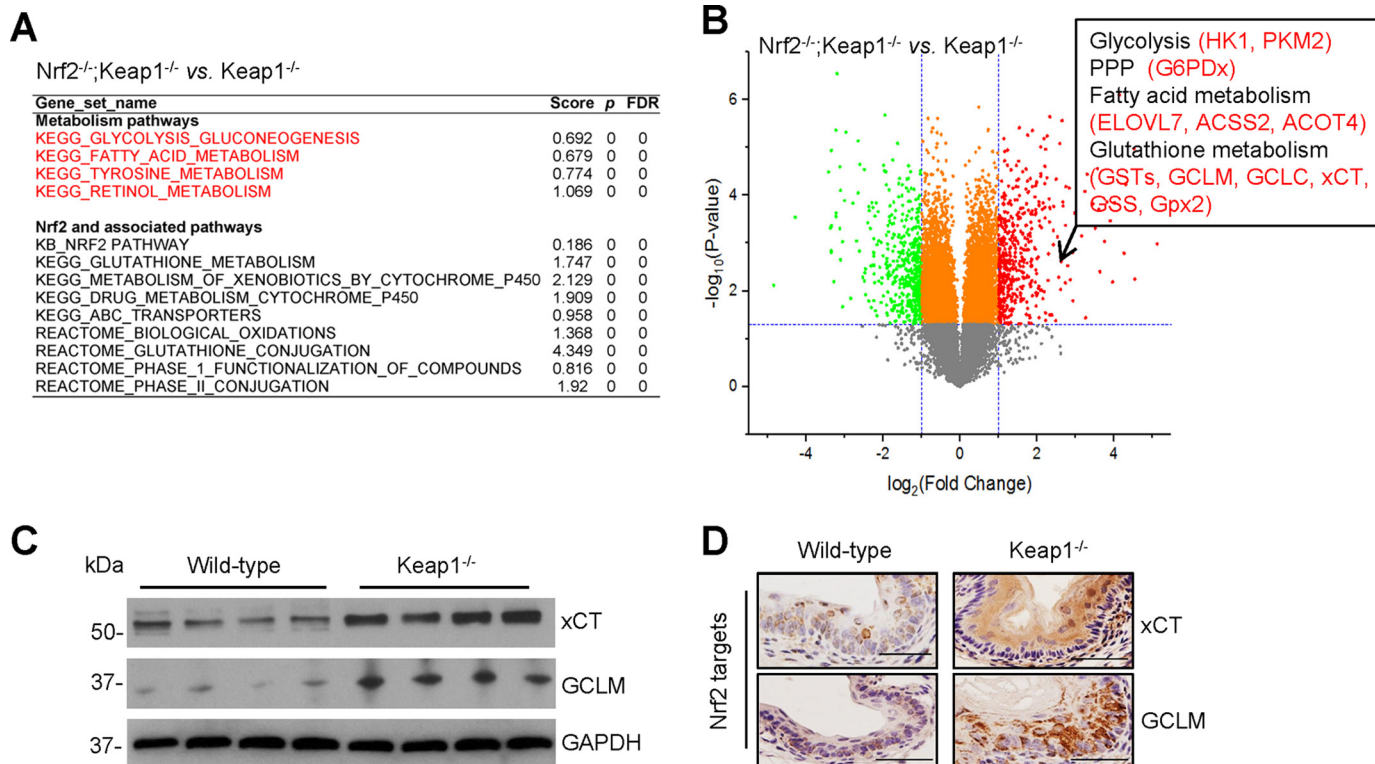


Figure 3. Differential expression of energy metabolism genes in Keap1^{-/-} esophagus. GSA analysis showed enrichment of four metabolic pathways in addition to classical Nrf2 pathways in Keap1^{-/-} esophagus ($n = 3$) as compared with Nrf2^{-/-};Keap1^{-/-} esophagus ($n = 3$) (A). Many metabolic genes were up-regulated as shown on the volcano graph (thresholds set at $p < 0.05$ and fold change > 2) after two-class SAM analysis. p values were determined using two-way ANOVA analysis (B). Differential expression of two canonical Nrf2 targeted genes in Keap1^{-/-} esophagus was validated by Western blotting (C) and IHC (D).

metabolism in Keap1^{-/-} esophagus suggested a good quality of our metabolomics data (Fig. 2C).

In addition, significant changes in heme metabolism were consistent with the known anti-oxidative function of Nrf2. Significant changes in lipid biosynthesis, β -oxidation, eicosanoids and endocannabinoids, and nucleotide biosynthesis in Keap1^{-/-} esophagus were consistent with the phenotype of esophageal hyperproliferation (File S3). These data demonstrated that hyperactive Nrf2 resulted in metabolic reprogramming in Keap1^{-/-} esophagus.

Hyperactive Nrf2 up-regulated metabolic genes in mouse esophagus

Gene microarray data from our previous experiment using Keap1^{-/-} and Nrf2^{-/-};Keap1^{-/-} esophagus at P7 were further analyzed for differential gene expression (34). Gene set analysis showed enrichment of 41 gene sets in Keap1^{-/-} esophagus among which four gene sets were metabolism pathways and nine were known Nrf2-associated pathways (Fig. 3A; File S4). Consistent with this observation, multiple metabolic genes involved in glycolysis (*Hk1* and *Pkm2*), PPP (*G6pdx*), fatty acid metabolism (*Elovl7*, *Acss2*, and *Acot4*), and GSH metabolism (*Gsts*, *Gclm*, *Gclc*, *xCT*, *Gss*, and *Gpx2*), were up-regulated in Keap1^{-/-} esophagus (Fig. 3B; File S5). Using two canonical Nrf2 target genes (*xCT* and *Gclm*), we confirmed overexpression of these genes in Keap1^{-/-} esophagus by Western blotting (Fig. 3C) and IHC (Fig. 3D).

Using Nrf2 ChIP-seq, we identified 1940 genes as potential Nrf2 target genes in mouse esophagus (File S6). Among these

genes, 10 participated in glycolysis, 4 in PPP, 3 in glycogenolysis, 6 in fatty acid metabolism, 3 in glutaminolysis, 1 in NADPH synthesis, and 21 in GSH metabolism (Table 1). Using IHC and Western blotting, we confirmed overexpression of glycolysis genes (*Hk1*, *Gpi1*, *Pfkfb2*, *Aldoa*, *Eno1*, and *Eno4*), PPP genes (*G6pd*, *Pgd*, *Tkt*, and *Taldo1*), and NADPH synthesis genes (*Idh1* and *Me2*) in Keap1^{-/-} esophagus as compared with WT esophagus (Fig. 4, A and B). Consistent with differential expression of individual genes, gene set analysis also showed enrichment of many metabolic gene sets, such as glycolysis and PPP (File S7; Fig. 5A). We further analyzed activities of the rate-limiting enzymes of glycolysis (HK and PK) and PPP (G6PD). Significantly higher activities of these enzymes were found in Keap1^{-/-} esophagus as compared with WT esophagus (Fig. 5, B–D). All these data suggested that hyperactive Nrf2 caused metabolic reprogramming through transcriptional regulation of metabolic genes, and metabolic reprogramming may potentially play a critical role in the esophageal phenotype (hyperproliferation and hyperkeratosis) of Keap1^{-/-} esophagus.

Nrf2 regulated the expression and function of Pkm2 in mouse esophagus

Because PK is a rate-limiting enzyme of glycolysis and Pkm was identified by Nrf2 ChIP-seq, ChIP-PCR was performed to validate binding of Nrf2 to the promoter of the mouse *Pkm* gene (Fig. 6A). The PKM gene is known to be alternatively spliced to generate transcripts encoding either PKM1 or PKM2, with PKM1 expressed in tissues with high catabolic demand such as

Table 1
Nrf2-regulated energy metabolism genes in mouse esophagus as identified by ChIP-seq

Pathway	Gene Name	Full Description	Distance to Start	Position	Wide-type AvgPeak	Nrf2 ^{-/-} AvgPeak	Keap1 ^{-/-} AvgPeak
Glycolysis	<i>Glut1</i>	solute carrier family 2 (facilitated glucose transporter), member 1	-2810, 182	upstream, in gene	6.00	3.50	21.00
	<i>HK1</i>	hexokinase 1	100100, 96932, 85764	in gene, in gene, in gene	4.67	4.33	27.00
	<i>HK2</i>	hexokinase 2	58070	downstream	2.00	1.00	14.00
	<i>Gpi1</i>	glucose phosphate isomerase 1	-3711, -3743	upstream, upstream	32.00	4.00	101.00
	<i>Pfkfb2</i>	6-phosphofructo-2-kinase/fructose-2,6-bisphosphatase 2	13013, 12197, 11621	in gene, in gene, in gene	4.67	7.33	16.00
	<i>Pfkfb4</i>	6-phosphofructo-2-kinase/fructose-2,6-bisphosphatase 4	17954	in gene	11.00	5.00	58.00
	<i>Aldoa</i>	aldolase A, fructose-bisphosphate	1503, 831	in gene, in gene	10.00	11.00	28.50
	<i>Eno1</i>	enolase 1, alpha non-neuron	2835	in gene	8.00	6.00	39.00
	<i>Eno4</i>	enolase 4	35551	downstream	10.00	3.00	43.00
	<i>Pkm</i>	pyruvate kinase, muscle	-2800, 2896	upstream, in gene	5.50	4.50	24.50
PPP pathway	<i>Tkt</i>	transketolase	15475, 15459	in gene, in gene	21.00	5.00	89.00
	<i>Pgd</i>	phosphogluconate dehydrogenase	-109, -4205	upstream, upstream	7.50	6.50	32.50
	<i>G6pdx</i>	glucose-6-phosphate dehydrogenase X-linked	4617, 3817	in gene, in gene	5.00	2.00	27.50
	<i>Taldo1</i>	transaldolase 1	896	in gene	8.00	2.00	44.00
Glycogenolysis	<i>Pgm5</i>	phosphoglucomutase 5	175282	in gene	7.00	2.00	14.00
	<i>Gbe1</i>	glucan (1,4-alpha-), branching enzyme 1	-583, 16697	upstream, in gene	7.50	6.50	32.00
	<i>Gaa</i>	glucosidase, alpha, acid	401	in gene	8.00	9.00	17.00
Fatty acid metabolism	<i>Elovl7</i>	ELOVL family member 7, elongation of long chain fatty acids (yeast)	14940	in gene	5.00	1.00	15.00
	<i>Fads1</i>	fatty acid desaturase 1	-9256	upstream	1.00	1.00	14.00
	<i>Acs2</i>	acyl-CoA synthetase short-chain family member 2	50021	downstream	4.00	3.00	12.00
	<i>Aco17</i>	acyl-CoA thioesterase 7	12348, 16892, 89836	in gene, in gene, in gene	7.33	4.00	17.00
	<i>Acad10</i>	acyl-Coenzyme A dehydrogenase family, member 10	41246	downstream	7.00	6.00	12.00
	<i>Acad12</i>	acyl-Coenzyme A dehydrogenase family, member 12	-326	upstream	7.00	6.00	12.00
Glutaminolysis	<i>Slc1A4</i>	solute carrier family 1 (glutamate/neutral amino acid transporter), member 4	7401	in gene	7.00	1.00	20.00
	<i>Gls2</i>	glutaminase 2 (liver, mitochondrial)	-8891	upstream	3.00	2.00	10.00
	<i>Gpi2</i>	glutamic pyruvate transaminase (alanine aminotransferase) 2	40295	downstream	7.00	1.00	28.00
NADPH synthesis	<i>Me1</i>	malic enzyme 1, NADP(+)-dependent, cytosolic	490	in gene	7.00	4.00	19.00
Glutathione metabolism	<i>Gsta4</i>	glutathione S-transferase, alpha 4	-158	upstream	8.00	2.00	67.00
	<i>Gsta3</i>	glutathione S-transferase, alpha 3	-173	upstream	6.00	3.00	35.00
	<i>Gstz1</i>	glutathione transferase zeta 1 (maleylacetoacetate isomerase)	131	in gene	6.00	7.00	17.00
	<i>Gstp1</i>	glutathione S-transferase, pi 1	-8232, -8, -8200	upstream, upstream, upstream	10.50	4.50	89.00
	<i>Gstp2</i>	glutathione S-transferase, pi 2	-3923, 4301, -3891	upstream, downstream, upstream	10.50	4.50	89.00
	<i>Gsta2</i>	glutathione S-transferase omega 2	19191	in gene	2.00	2.00	14.00
	<i>Mgst2</i>	microsomal glutathione S-transferase 2	9687	in gene	5.00	1.00	20.00
	<i>Gstm7</i>	glutathione S-transferase, mu 7	-7935	upstream	6.00	7.00	42.00
	<i>Gstm6</i>	glutathione S-transferase, mu 6	4069	in gene	6.00	7.00	42.00
	<i>Gstm3</i>	glutathione S-transferase, mu 3	4230	in gene	8.00	2.00	35.00
	<i>Gstm2</i>	glutathione S-transferase, mu 2	271	in gene	4.00	1.00	12.00
	<i>Gstm1</i>	glutathione S-transferase, mu 1	4469, 4565	in gene, in gene	22.00	4.00	43.00
	<i>Gclm</i>	glutamate-cysteine ligase, modifier subunit	-1912	upstream	5.00	2.00	28.00
	<i>Gclc</i>	glutamate-cysteine ligase, catalytic subunit	-3895, -9439, -3911	upstream, upstream, upstream	13.50	4.00	56.50
	<i>xCT</i>	solute carrier family 7 (cationic amino acid transporter, y+ system), member 11	6941, 5373, -83	in gene, in gene, upstream	3.67	3.67	29.67
	<i>Gss</i>	glutathione synthetase	24642, 7170, 1698, 130	in gene, in gene, in gene, in gene	4.50	5.50	16.50
	<i>Gpx2</i>	glutathione peroxidase 2	66	in gene	3.00	3.00	26.00
	<i>Gpx4</i>	glutathione peroxidase 4	-1350	upstream	10.00	8.00	28.00
	<i>Gsr</i>	glutathione reductase	122, 714	in gene, in gene	5.50	3.50	27.00
	<i>Sod1</i>	superoxide dismutase 1, soluble	-38, 634	upstream, in gene	8.00	7.00	16.00
<i>Cat</i>	catalase	4737	in gene	9.00	3.00	71.00	

muscle and PKM2 in most adult tissues and cancer. Using Western blotting, we confirmed overexpression of Pkm2, but not Pkm1, in *Keap1^{-/-}* esophagus (Fig. 6B). IHC showed that Pkm2 was overexpressed in squamous epithelial cells, whereas Pkm1 was expressed in smooth muscle cells (Fig. 6C).

To explain why hyperactive Nrf2 selectively up-regulated Pkm2 expression, we examined the expression of hnRNPA1, hnRNPA2, RBM4, and PTB, which were known to regulate alternative splicing of the *Pkm* gene (35, 36). As expected, the *Keap1^{-/-}* esophagus expressed higher levels of hnRNPA1, hnRNPA2, and PTB and a lower level of RBM4 than WT esophagus (Fig. 6D).

An overall increase in nucleotide-sugar and amino-sugar metabolism in *Keap1^{-/-}* esophagus suggested that glycosylation may be enhanced by hyperactive Nrf2. Indeed, there was an increase in protein glycosylation in the *Keap1^{-/-}* esophagus. Pkm2 glycosylation was also enhanced as detected by Pkm2 Western blotting after immunoprecipitation with anti-O-GlcNAc (Fig. 6E). Pkm2 exists in a mixture of monomer, dimer, and tetramer with the tetramer being the most enzymatically active form. Although all three forms of Pkm2 were increased in *Keap1^{-/-}* esophagus, a dramatic increase of tetrameric Pkm2 suggested an increase of glycolysis and subsequent increase in ATP production in the mitochondria (Fig. 6F). As expected, ATP biosynthesis was increased as well (Fig. 6G).

Pkm2 knockout failed to inhibit esophageal phenotype in *Keap1^{-/-}* mice

To further test the role of Pkm2 in hyperactive Nrf2-mediated esophageal phenotype in *Keap1^{-/-}* esophagus, we generated *K5Cre;Pkm2^{fl/fl};Keap1^{-/-}* mice to constitutively knock out *Pkm2* in esophageal squamous epithelial cells *in vivo*. To our surprise, *Pkm2* knockout did not significantly modify PCNA expression, BrdU incorporation, and the expression of squamous differentiation markers (Krt5, Krt1, and loricrin) (Fig. 7A). Instead, Pkm1 was overexpressed in the esophageal squamous epithelial cells of *K5Cre;Pkm2^{fl/fl};Keap1^{-/-}* esophagus as a result of *Pkm2* knockout.

Nrf2 knockdown, *Pkm2* knockdown, and glycolysis inhibitors suppressed the proliferation of NRF2^{high} human ESCC cells *in vitro*

We next sought to determine the transient effects of NRF2 or PKM2 inhibition on the proliferation of esophageal squamous epithelial cells. Human ESCC cells, KYSE510 and KYSE450, both express a low level of NRF2 (NRF2^{low} cells), and KYSE70 expresses a high level of NRF2 due to a point mutation of the *NRF2* gene (NRF2^{high} cells) (37–39). KYSE450 cells (NRF2^{low}) and KYSE70 cells (NRF2^{high}) were transfected with siRNAs and/or treated with glycolysis inhibitors, 2DG (HK inhibitor) (40) and shikonin (PKM2 inhibitor) (41). NRF2^{low} cells were treated with *KEAP1* siRNA to activate NRF2. Transfection effi-

Hyperactive Nrf2 in the esophagus

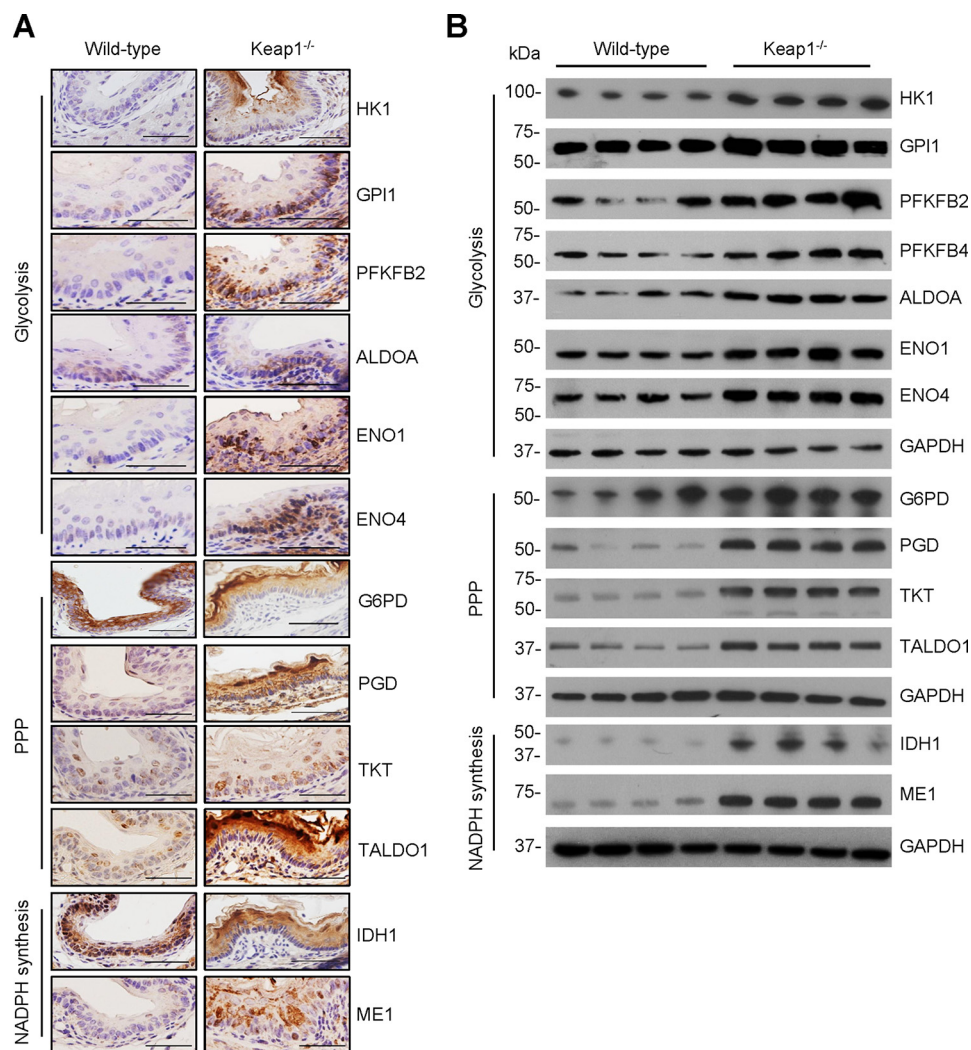


Figure 4. Hyperactive Nrf2 up-regulated the expression of metabolic genes in mouse esophagus. IHC (A) and Western blotting (B) confirmed overexpression of glycolysis genes, PPP genes, and NADPH synthesis genes in *Keap1*^{-/-} esophagus as compared with WT esophagus. Scale bar, 50 μ m.

ciency was determined by Western blotting (Fig. 8, A and E), cell proliferation by colony formation assay (Fig. 8, B, F, D, and H), and ATP biosynthesis (Fig. 8, C and G). *NRF2* knockdown, *PKM2* knockdown, and glycolysis inhibitors suppressed cell proliferation and ATP biosynthesis in both cells *in vitro*. Similar results were found in KYSE510 cells (data not shown). Consistent with the *in vivo* data, *PKM2* siRNA knockdown resulted in up-regulation of *PKM1* (Fig. 8A, lane 3 versus lane 1, lane 5 versus lane 2; and E, lane 2 versus lane 1).

Discussion

This study clearly demonstrated that hyperactive Nrf2 causes metabolic reprogramming through transcriptional regulation of metabolic genes in mouse esophagus. To our knowledge, it is the first study to demonstrate that hyperactive Nrf2 differentially up-regulated the *Pkm2* isoform in the esophageal squamous epithelial cells *in vivo*. However, constitutive *Pkm2* knockout in the mouse esophagus failed to inhibit the esophageal phenotype in *Keap1*^{-/-} mice.

NRF2 signaling pathway has been reported to regulate energy metabolism. In A549 cells (a lung cancer cell line with hyperactive NRF2), NRF2 was found to regulate the expression

of metabolic genes involved in PPP, nucleotide synthesis, and NADPH synthesis. Metabolic pathways such as glycolysis, PPP, glutaminolysis were subject to NRF2 regulation as well (42). Similar results were observed in mouse forestomach when Nrf2 became hyperactive due to *Keap1* knockout (42). In a transgenic mouse line with constitutively active Nrf2, Nrf2 activation in mouse skin was found to cause significant alterations in metabolic pathways of GSH, purine, and amino acid, PPP, citric acid cycle, and glycolysis (43). NRF2 activation by phosphomimetic P62 up-regulated metabolic genes and thus enhanced GSH production and several metabolic pathways in human liver cells (44). In addition, NRF2 also regulated serine biosynthesis (45) and lipid metabolism (46). However, careful examination of the metabolomics data of ours and others showed that metabolic pathways regulated by hyperactive NRF2 depended on the cellular or tissue context (44, 47). For example, a *Keap1* knockout in skeletal muscle cells *in vivo* up-regulated metabolic genes of glycogenolysis (*Gbe1* and *Phka1*). However, its regulation of glycogen metabolism was different in the liver potentially because of the different enzyme makeup in these tissues (47). Metabolism in cul-

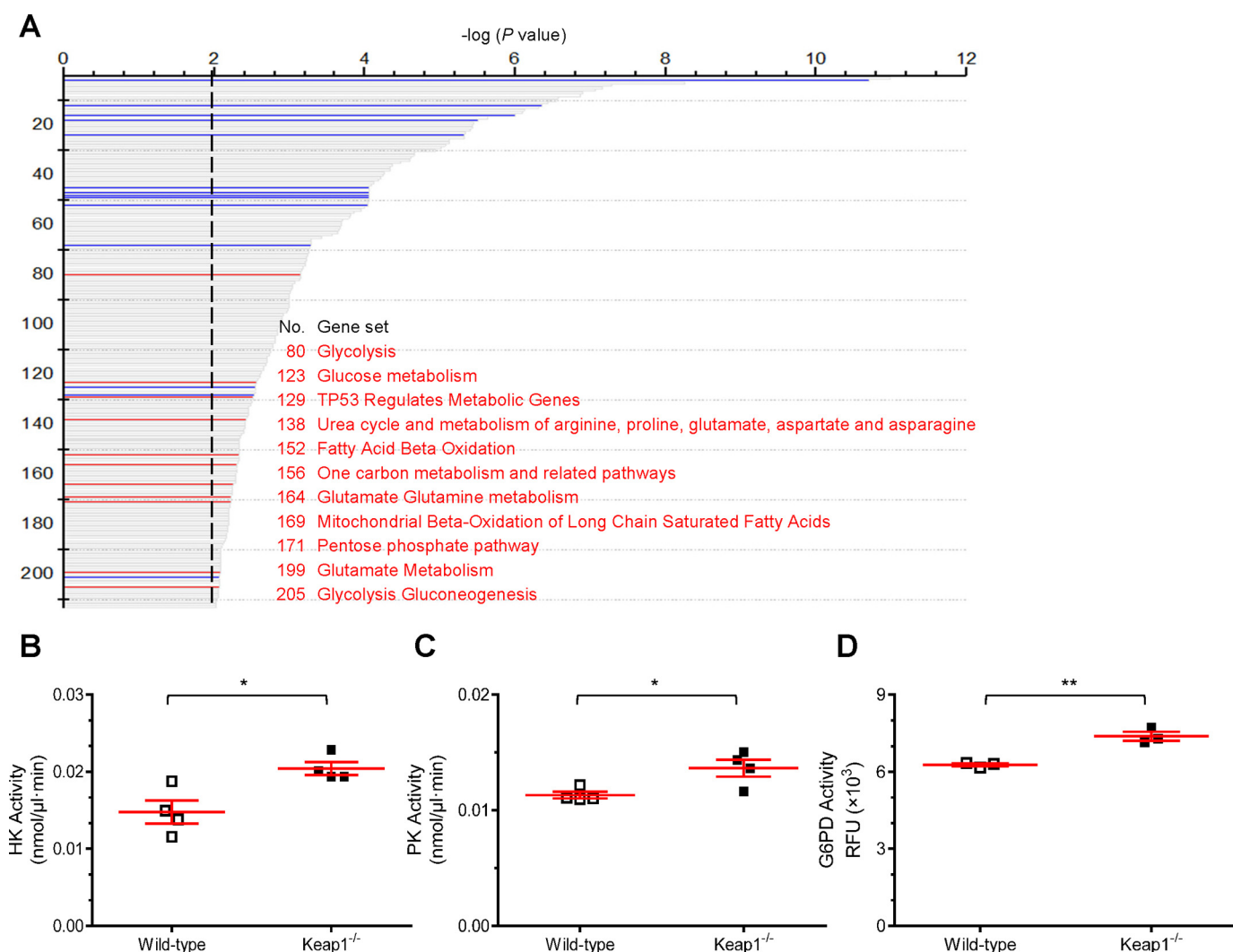


Figure 5. ChIP-seq identified metabolic genes regulated by Nrf2 in mouse esophagus. GSA of ChIP-seq gene shows 11 metabolic gene sets by comparing *Keap1*^{-/-} esophagus ($n = 4$) with WT esophagus ($n = 4$) (threshold set at $p < 0.01$). p values were determined using two-way ANOVA analysis (A). Enzymatic activities of HK (B), PK (C), and G6PD (D) were increased in *Keap1*^{-/-} esophagus ($n = 4$) as compared with WT esophagus ($n = 4$). *, $p < 0.05$; **, $p < 0.01$. p values were determined using Student's t test.

tured cells and live tissues responded to genetic or pharmacological manipulation of NRF2 signaling differently because of their differential nutrient use (48). Thus, there is a need to understand the role of NRF2 in metabolism in specific cellular or tissue context. Our data clearly showed that many metabolic pathways were impacted by hyperactive Nrf2 in mouse esophagus (Fig. 2). Consistent with metabolic changes, the expression of many metabolic genes was up-regulated (Fig. 4), and the activities of three enzymes (HK, PK, and G6PD) were enhanced (Fig. 5). In addition to the classical Warburg effect (aerobic glycolysis), hyperactive Nrf2, in fact, impacted oxidative phosphorylation in the esophagus as well, consistent with a current model of cancer metabolism (49). Our results support the notion that Nrf2 regulates mitochondrial fatty acid oxidation, respiration, and ATP biogenesis (50). In fact, gene sets associated with oxidoreductase activity, mitochondrial biogenesis, and energy metabolism were down-regulated in the *Nrf2*^{-/-} esophagus, as well as ATP biogenesis and CoxIV (28). A recent study further demonstrated that hyperactive NRF2 increased proteasome activity through transcriptional up-regulation of

proteasome genes, enhanced degradation of the mitochondrial fission protein DRP1, and thus promoted mitochondrial hyperfusion to generate more ATP, produce fewer reactive oxygen species, and make cells more resistant to apoptosis (51). The antioxidative function of NRF2 clearly outweighs the oxidative stress generated by oxidative phosphorylation. As a consequence, reactive oxygen species and oxidative damages were suppressed by hyperactive NRF2 both *in vitro* and *in vivo* (52–54).

In addition to its nonmetabolic functions, PKM2 has also been regarded as an important player in aerobic glycolysis and the growth of cancer cells (48, 55). Almost universal expression of PKM2 in rapidly proliferating cells suggests that PKM2 expression is permissive to the metabolic requirements of proliferation (56). In addition to its transcriptional regulation, PKM2 was also subject to regulation by O-GlcNAcylation and polymerization (57). In this study, hyperactive Nrf2 was found to up-regulate Pkm2 expression through transcriptional regulation and alternative splicing of *Pkm* gene in mouse esophagus (Fig. 6).

Hyperactive Nrf2 in the esophagus

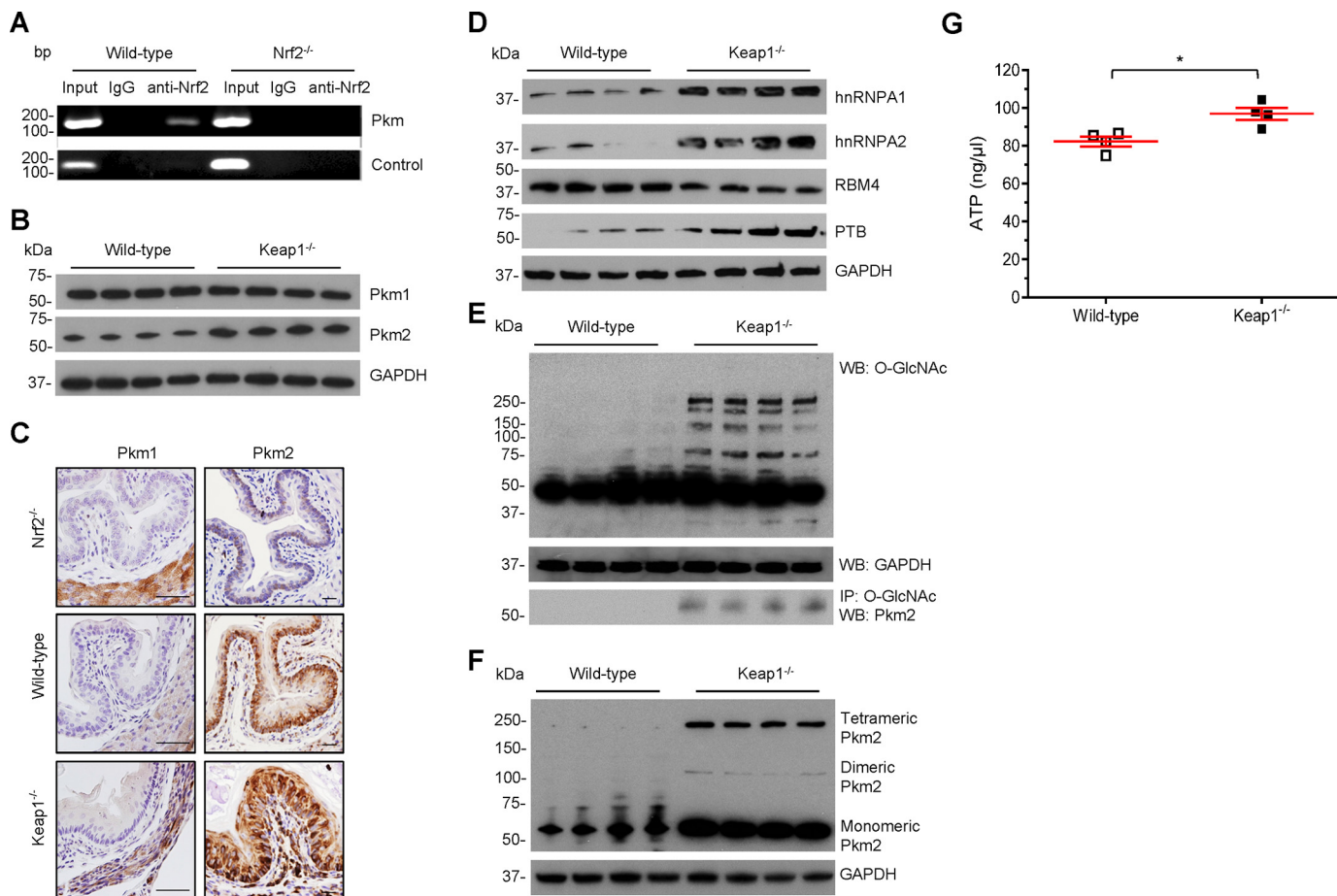


Figure 6. Hyperactive Nrf2 regulated the expression and function of key metabolic genes for ATP biosynthesis in mouse esophagus. ChIP-PCR shows Nrf2 protein bound to mouse *Pkm* sequence (A). Western blotting (B) and IHC (C) showed that hyperactive Nrf2 up-regulated Pkm2, but not Pkm1, in *Keap1*^{-/-} esophagus ($n = 4$ /group). Hyperactive Nrf2 up-regulated hnRNPA1, hnRNPA2, and PTB and down-regulated RBM4 to promote alternative splicing of the *Pkm* gene ($n = 4$ /group) (D). Meanwhile, protein O-GlcNAcylation, especially Pkm2 glycosylation (E), and Pkm2 tetramerization were increased in the *Keap1*^{-/-} esophagus as compared with the WT esophagus ($n = 4$ /group) (F). Consistent with these changes, ATP biosynthesis was up-regulated as shown by an ATP bioluminescent assay ($n = 4$ /group) (G). Scale bar, 50 μ m; *, $p < 0.05$. p values were determined using Student's t test.

The net effect of PKM2 inhibition may depend on the cellular context. Fast-growing cells may rely more on PKM2 to regulate their PK activity to support anabolic metabolism. Replacing PKM2 with PKM1 results in loss of flexibility to tune PK activity that is critical for such fast-growing cells. Slow-growing cells may not have such a dependence (58). Our data showed that constitutive *Pkm2* knockout had no effect on the esophageal phenotype *in vivo*. This may be explained by several possibilities. 1) Permanent *Pkm2* knockout can be compensated by Pkm1 overexpression (Fig. 7A). In fact, Pkm1 overexpression has been observed in *Pkm2* knockout cells or tissues in multiple studies *in vitro* (58, 59) and *in vivo* (60, 61). Pkm1 overexpression is due to transcriptional up-regulation, although the possibility of post-transcriptional regulation cannot be excluded. It has been shown in the literature that germline or conditional loss of *Pkm2* *in vivo* not only reduced the mRNA levels of *Pkm2* and total *Pkm*, but also increased the mRNA level of *Pkm1* in multiple mouse tissues, bone marrow hematopoietic cells, mammary tumor cells, and sarcoma cells (2, 58, 60, 62, 63). Blocking glycolysis may be compensated by increased serine and glycine biosynthesis from both glucose and glutamine (64). Two recent studies have shown that hyperactive NRF2 in cancer cells resulted in energy dependence on glutaminolysis and

inhibition of glutaminase suppressed cancer cell growth (65, 66). Indeed, glutamate level was significantly higher in the *Keap1*^{-/-} esophagus than the WT esophagus. Consistent with this, glutaminase 2 was overexpressed in the *Keap1*^{-/-} esophagus as detected by IHC and Western blotting (Fig. 7, B–D) (3). Many factors other than oncogenes, for example tissue type (*e.g.* cell lineage and environment) and interactions with benign cells, contribute to the metabolic phenotype of cancers (48, 67).

Nevertheless, transient inhibition of PKM2 by siRNA knock-down and shikonin *in vitro* suppressed cell proliferation and ATP biosynthesis in human ESCC cells, albeit compensative overexpression of PKM1 (Fig. 8). These data suggest that in the clinical setting where transient inhibition is desirable, PKM2 inhibition remains a promising approach for therapy of NRF2^{high} ESCC. To fully elucidate the functional role of PKM2 in NRF2^{high} ESCC, we have developed a mouse line carrying a knockin floxed mutant *Nrf2* allele, which allows conditional activation of Nrf2 signaling when crossed with an esophageal epithelium-specific *Cre* line.⁵ Strong esophageal phenotypes, hyperproliferation and hyperkeratinization, developed at 4

⁵ C. Paiboonrungruan and X. Chen, unpublished data.

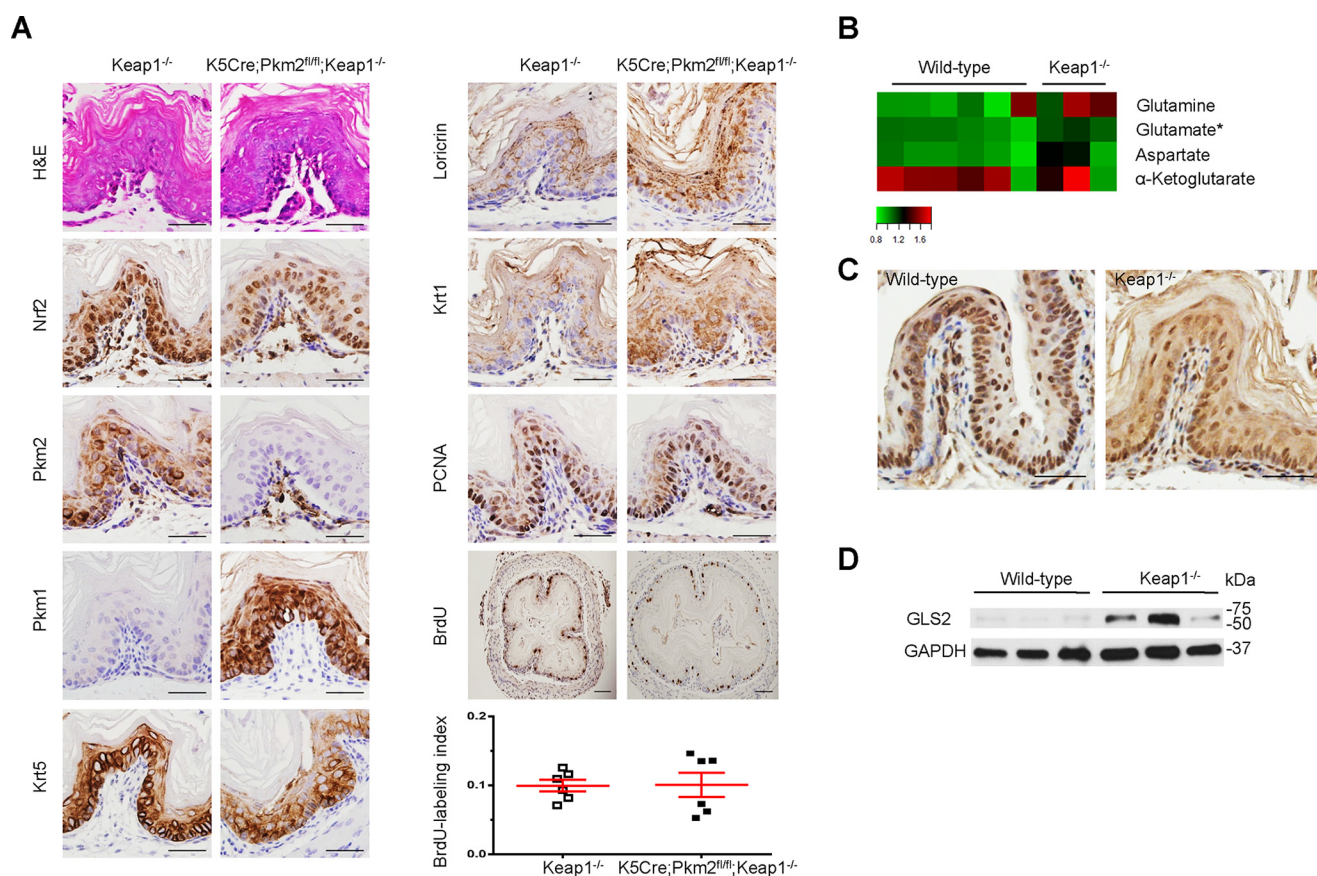


Figure 7. Constitutive Pkm2 knockout in the esophagus failed to inhibit hyperproliferation and hyperkeratosis of *Keap1*^{-/-} esophagus *in vivo*. As compared with *Keap1*^{-/-} esophagus, *Pkm2* knockout did not significantly change the general morphology (hematoxylin and eosin staining), the expression of differentiation markers (Krt5, loricrin, and Krt1), and the expression of proliferation markers (PCNA, BrdU, and BrdU-labeling index). Although *Pkm2* was completely silenced in the esophageal squamous epithelial cells of the *K5Cre;Pkm2*^{fl/fl};*Keap1*^{-/-} esophagus, *Pkm1* expression was dramatically up-regulated as compared with *Keap1*^{-/-} esophagus (A). Glutamate level was significantly higher in the *Keap1*^{-/-} esophagus ($n = 3$) than the WT esophagus ($n = 6$) (B). *, $p < 0.05$. p values were determined using Student's t test. Consistent with this, glutaminase 2 was overexpressed in *Keap1*^{-/-} esophagus as detected by IHC and Western blotting ($n = 3$ /group) (C and D). Scale bar, 50 μ m.

weeks after tamoxifen induction. (unpublished preliminary data). This line will be crossed with *Pkm2*^{fl/fl} mice to determine whether conditional blockage of *Pkm2* may inhibit the esophageal phenotype due to hyperactive Nrf2, at least in a short term.

It should be noted that our study has one limitation. The whole esophagus (epithelium and muscle) instead of the epithelium alone was used for metabolomic profiling, Western blotting, and enzyme activity assays in this study. This is due to a practical limitation that all *Keap1*^{-/-} mice die within 3 weeks after birth (18). We harvested mouse esophagus from P7 mice when mice are healthy yet the esophagus is tiny. At this age, it is impractical to harvest enough epithelium from *Keap1*^{-/-} mice. To overcome this limitation, in addition to experiments using the whole esophagus, we used immunohistochemistry to validate differential expression of metabolic genes in esophageal squamous epithelial cells *in vivo* (Figs. 3, 4, and 6).

In summary, we characterized metabolomic reprogramming and differential gene expression in mouse esophagus due to hyperactive Nrf2. Our data pointed out metabolic pathways (e.g. glycolysis and oxidative phosphorylation) and genes (e.g. *Pkm2*) as downstream targets. Further studies are warranted to find out how to inhibit the esophageal phenotype in the

NRF2^{high} esophagus and translate the discovery for targeted therapy of NRF2^{high} ESCC.

Experimental procedures

Animal experiment

Animal experiments were approved by the Institutional Animal Care and Use Committees at the North Carolina Central University (protocol number XC-12-03-2008). Animals in these experiments were bred and maintained at the local animal facility according to local legislation. WT C57BL/6J mice were purchased from The Jackson Laboratory (Bar Harbor, ME). *Nrf2*^{-/-} and *Keap1*^{-/-} mice on the C57BL background were obtained from the Experimental Animal Division, RIKEN BioSource Center (Tsukuba, Japan) (18). *K5Cre* mice (68), *Pkm2*^{fl/fl} mice (60) (The Jackson Laboratory), and *Keap1*^{-/-} mice were crossed to generate *K5Cre;Pkm2*^{fl/fl};*Keap1*^{-/-} mice. Mouse esophagus at P7 was harvested for analysis of metabolomics, Nrf2 ChIP-seq, morphology, and gene expression. BrdU (50 mg/kg, i.p.) was given to some mice 2 h before sacrifice.

Metabolomic profiling

Three groups of mouse esophageal tissue samples, six of each genotype (*Nrf2*^{-/-}, WT, and *Keap1*^{-/-}), were analyzed by a

Hyperactive Nrf2 in the esophagus

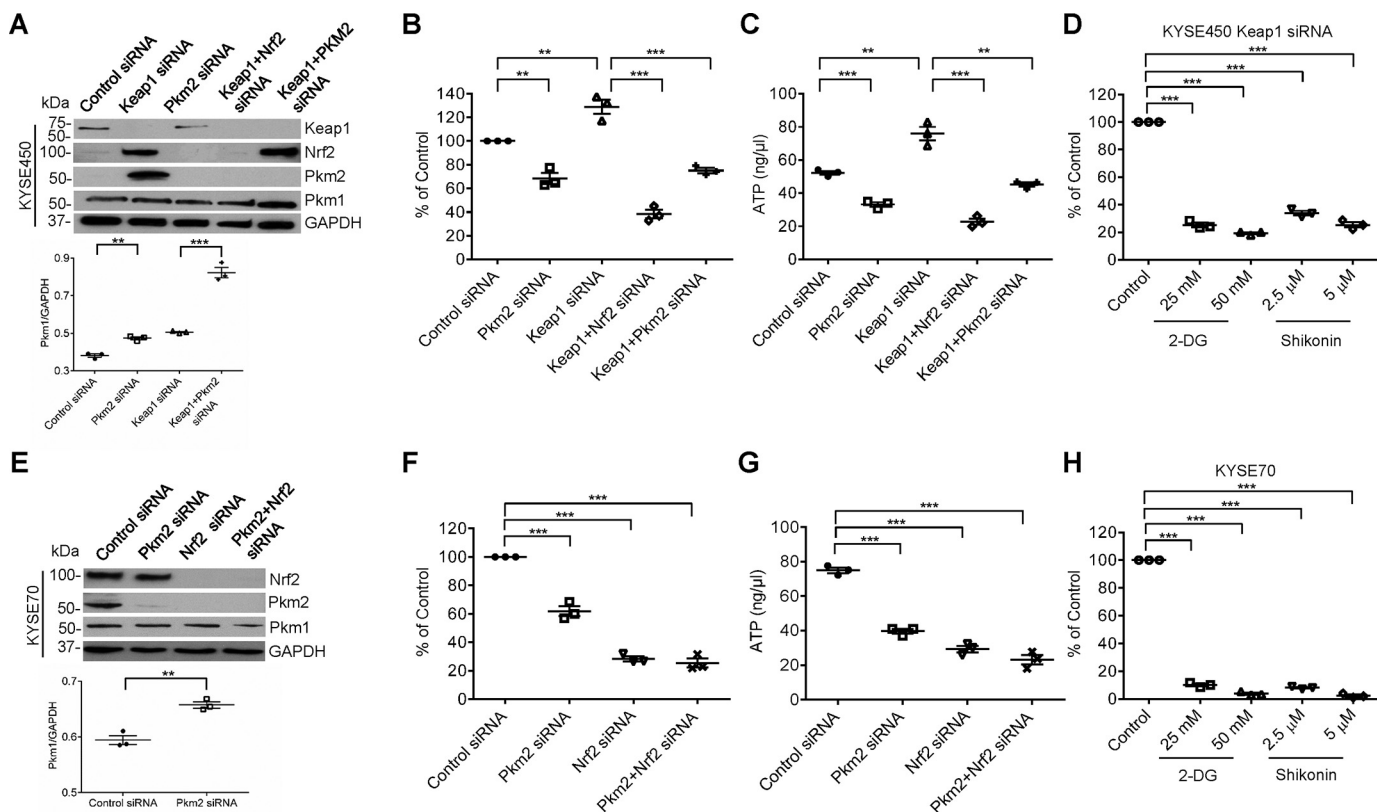


Figure 8. Transient inhibition of glycolysis suppressed colony formation and ATP biosynthesis of ESCC cells *in vitro*. KYSE450 cells ($NRF2^{low}$) and KYSE70 cells ($NRF2^{high}$) were transfected with siRNA or treated with glycolysis inhibitors, 2DG (HK inhibitor) and shikonin (PKM2 inhibitor). Transfection efficiency and PKM1/GAPDH were determined by Western blotting (A and E), cell proliferation by colony formation assay (B, F, D, and H), and ATP biosynthesis by a bioluminescent assay (C and G) ($n = 3$). *, $p < 0.05$; **, $p < 0.01$; ***, $p < 0.001$. p values were determined using Student's t test.

biochemical profiling platform (Metabolon Inc, Durham, NC) with ultrahigh performance LC-tandem MS (File S2 and S3). $Keap1^{-/-}$ esophagus was much smaller than others and two esophagi were pooled together to make one sample for the analysis. Raw data were extracted, peak-identified and QC processed by Metabolon. Refined data were analyzed by two-way ANOVA with SPSS and plotted with GraphPad. Heatmap was generated using R (gplots package).

Histochemical staining and IHC

Hematoxylin and eosin staining was conducted based on a routine protocol. For IHC staining, deparaffinized sections were pre-treated to retrieve antigens using a Tris-based Antigen Unmasking Solution (Vector Laboratories, Burlingame, CA), prior to incubation with an antibody overnight at 4 °C. Detection of the antibody complex was done using the streptavidin-peroxidase reaction kit with 3,3'-diaminobenzidine as a chromogen (ABC kit, Vector Labs) (Table 2). BrdU-labeling index was calculated by dividing the number of BrdU⁺ epithelial cells with the total number of epithelial cells in the esophagus. Three cross-sections of each mouse esophagus were stained for BrdU and counted.

Western blotting

Protein was isolated from mouse tissues using a standard method. In brief, tissue lysates were prepared by homogenizing tissue with the TissueLyser bead mill (Qiagen, Valencia, CA) in

RIPA buffer. Cell debris was removed by a short centrifugation, and an aliquot of cleared lysate was kept for protein quantitation using the BCA protein assay kit (Bio-Rad). Protein samples were separated by SDS-PAGE, and transferred to a nitrocellulose membrane (Millipore, Billerica, MA). After blocking with 5% nonfat dry milk, the membrane was probed with an antibody at 4 °C overnight (Table 2). Immunoreactivity was visualized by applying HRP ECL substrate and immediately exposing the membranes to film. The blots were stripped and re-probed for GAPDH.

ChIP-seq and ChIP-PCR

Nrf2 ChIP-seq was conducted by Active Motif (Carlsbad, CA) using a ChIP-seq validated antibody (sc-13032, Santa Cruz Biotechnology) and three mouse esophageal tissue samples, one of each genotype ($Nrf2^{-/-}$, WT, and $Keap1^{-/-}$) (GSE122504). The quality of ChIP DNA was controlled by quantitative PCR of two positive control genes ($Nqo1$ and $Txnrd1$) and a negative control ($Ccnt1$). Enriched genes in $Keap1^{-/-}$ esophagus as compared with $Nrf2^{-/-}$ and WT samples were regarded as potential Nrf2 target genes. This gene list was further analyzed for gene sets using an on-line tool (<http://cpdb.molgen.mpg.de/>)⁶ (70, 71).

⁶ Please note that the JBC is not responsible for the long-term archiving and maintenance of this site or any other third party hosted site.

Table 2
Antibody information

Antigen	Test sample	Dilution in IHC	Dilution in WB	Cat#	Host	Mono/Poly	Company	City/State
Eno4	Mouse tissue	1:20	1:200	ab204433	Rb	Poly	Abcam	Cambridge, MA
Gpi1	Mouse tissue	1:500	1:1000	ab66340	Ms	Mono	Abcam	Cambridge, MA
G6pd	Mouse tissue	1:500	1:1000	ab76598	Rb	Poly	Abcam	Cambridge, MA
Gclm	Mouse tissue	1:50	1:1000	ab126704	Rb	Mono	Abcam	Cambridge, MA
Eno1	Mouse tissue	1:50	1:1000	ab193111	Rb	Poly	Abcam	Cambridge, MA
Tkt	Mouse tissue	1:50	1:1000	sc-67120	Rb	Poly	Santa Cruz	Dallas, TX
Idh1	Mouse tissue	1:50	1:1000	ab172964	Rb	Mono	Abcam	Cambridge, MA
Me1	Mouse tissue	1:50	1:1000	ab97445	Rb	Poly	Abcam	Cambridge, MA
Pkm2	Mouse tissue	1:400	1:1000	4053s	Rb	Mono	Cell Signaling	Danvers, MA
Pgd	Mouse tissue	1:25	1:1000	ab175116	Rb	Poly	Abcam	Cambridge, MA
Taldo1	Mouse tissue	1:25	1:1000	ab137629	Rb	Poly	Abcam	Cambridge, MA
xCT	Mouse tissue	1:200	1:1000	PA1-16893	Rb	Poly	Thermo	Waltham, MA
Pkm1	Mouse tissue	1:200	1:1000	7067s	Rb	Mono	Cell Signaling	Danvers, MA
Hk1	Mouse tissue	1:100	1:1000	ab110529	Rb	Poly	Abcam	Cambridge, MA
Pfkfb2	Mouse tissue	1:100	1:1000	GTX55273	Rb	Poly	GeneTex	Irvine, CA
Aldoa	Mouse tissue	1:100	1:1000	ab169544	Rb	Mono	Abcam	Cambridge, MA
hnRNPA1	Mouse tissue	-	1:1000	ab5832	Ms	Mono	Abcam	Cambridge, MA
hnRNPA2	Mouse tissue	-	1:1000	ab31645	Rb	Poly	Abcam	Cambridge, MA
Rbm4	Mouse tissue	-	1:1000	ab154760	Rb	Poly	Abcam	Cambridge, MA
Ptb	Mouse tissue	-	1:1000	ab133734	Rb	Mono	Abcam	Cambridge, MA
Keap1	Mouse tissue	-	1:1000	ab66620	Rb	Poly	Abcam	Cambridge, MA
O-GlcNAc	Mouse tissue	-	1:1000	MABS1254	Ms	Mono	EMD Millipore	Temecula, CA
Pfkfb4	Mouse tissue	-	1:1000	GTX107755	Rb	Poly	GeneTex	Irvine, CA
Gapdh	Mouse tissue	-	1:5000	ab8245	Ms	Mono	Abcam	Cambridge, MA
Pcna	Mouse tissue	1:800	-	P8825	Ms	Mono	Sigma Aldrich	St. Louis, MO
Loricrin	Mouse tissue	1:500	-	ab85679	Rb	Poly	Abcam	Cambridge, MA
BrdU	Mouse tissue	1:500	-	ab6326	Rat	Mono	Abcam	Cambridge, MA
Krt5	Mouse tissue	1:200	-	RM-2166-S0	Rb	Mono	Thermo	Waltham, MA
Krt1	Mouse tissue	1:200	-	ab93652	Rb	Poly	Abcam	Cambridge, MA
Nrf2	Mouse tissue	1:400	1:1000	-	Rb	Poly	Provided by Dr. Edward E. Schmidt, Univ of Montana	-
Gls2	Mouse tissue	1:400	1:1000	ab113509	Rb	Poly	Abcam	Cambridge, MA

Nrf2-binding sites within the DNA sequence of mouse *Pkm* gene (ENSMUSG00000032294) were predicted using Anchored Combination TFBS Cluster Analysis (oPOSSUM version 3.0) (69). ChIP analysis was performed using an EZ-ChIP kit (Millipore, Billerica, MA) according to the manufacturer's instructions with the anti-Nrf2 used for ChIP-seq. Immunoprecipitated DNA or input was PCR-amplified with the following primer pairs: *Pkm* (5'-CTT-CCTATCCTCGGTAGTTTTCCAT-3' and 5'-CAGAATAATTC-TGTGATCCGTGAGA-3'; predicted size = 177 bp); negative control (5'-GGTATGATGACAACCACCTTTACG-3' and 5'-AAACCTCAGTCGCTGGACCAAGAC-3'; predicted size = 155 bp).

Analysis of gene microarray data

Microarray data of two GEO datasets, GSE34278 (*Nrf2*^{-/-}; *Keap1*^{-/-} mouse esophagus versus *Keap1*^{-/-} mouse esophagus) and GSE23400 (53 cases of human ESCC), were analyzed. Differentially expressed genes were obtained from two-class significance analysis of microarrays (SAM) in Excel with the median number of false positives less than 1 (34). GSA was carried out using R (GSA package). Mouse data were obtained from our previous study on mouse esophagus at P7 (34). Hierarchical clustering analysis was performed using the R package. Volcano graph was generated with Origin software (Volcano-Plot package, OriginLab, Northampton, MA).

Enzymatic activity and ATP

HK activity (MAK091, Sigma), PK activity (MAK072, Sigma), G6PD activity (12581, Cell Signaling), and ATP (MAK190, Sigma) were analyzed according to the manufacturer's instructions of the kits.

Cell culture and treatment

Human ESCC cells, KYSE510 (NRF2^{low}), KYSE450 (NRF2^{low}), and KYSE70 (NRF2^{high}), were obtained from the ATCC (Manassas, VA) and ECACC (Porton Down, Salisbury, UK). NRF2 hyperactivation in KYSE70 cells was due to a homozygous point mutation of the *NRF2* gene (W24C) (37–39). KYSE510, KYSE450, and KYSE70 cells were exposed to 2DG (Sigma), shikonin (Sigma), or transfected with siRNAs (ThermoFisher Scientific, Waltham, MA) using Lipofectamine RNAiMAX (Invitrogen) according to the manufacturer's instructions. All cell culture experiments were triplicated.

Statistical analyses

GraphPad Prism 6 (GraphPad Software, La Jolla, CA) was used for Student's *t* test. SPSS was used for two-way ANOVA analysis. *p* < 0.05 was considered statistically significant.

Author contributions—J. F., Z. X., C. H., J. L., Y. H., X. K., and X. L. C. data curation; J. F., Z. X., and C. H. software; J. F., Z. X., C. H., J. L., W. Y., Y. H., K. C., X. K., and X. L. C. formal analysis; J. F., Z. X., C. H., J. L., C. P., X. K., and X. L. C. investigation; J. F., Z. X., X. K., and X. L. C. methodology; J. F., Z. X., M. B. M., X. K., and X. L. C. writing-original draft; J. F., Z. X., M. B. M., X. K., and X. L. C. writing-review and editing; J. L., W. Y., Y. H., C. P., and K. C. validation; X. K. and X. L. C. conceptualization; X. K. and X. L. C. supervision; X. K. and X. L. C. project administration.

References

- Siegel, R. L., Miller, K. D., and Jemal, A. (2017) Cancer statistics, 2017. *CA Cancer J. Clin.* **67**, 7–30 [CrossRef Medline](#)
- Wu, X., Chen, V. W., Andrews, P. A., Ruiz, B., and Correa, P. (2007) Incidence of esophageal and gastric cancers among Hispanics, non-Hispanic whites and non-Hispanic blacks in the United States: subsite and histology differences. *Cancer Causes Control* **18**, 585–593 [CrossRef Medline](#)
- Du, P., Huang, P., Huang, X., Li, X., Feng, Z., Li, F., Liang, S., Song, Y., Stenvang, J., Brünner, N., Yang, H., Ou, Y., Gao, Q., and Li, L. (2017) Comprehensive genomic analysis of oesophageal squamous cell carcinoma reveals clinical relevance. *Sci. Rep.* **7**, 15324 [CrossRef Medline](#)
- Ma, S., Paiboonrungruan, C., Yan, T., Williams, K. P., Major, M. B., and Chen, X. L. (2018) Targeted therapy of esophageal squamous cell carcinoma: the NRF2 signaling pathway as target. *Ann. N.Y. Acad. Sci.* 2018 [CrossRef](#)
- Kensler, T. W., Wakabayashi, N., and Biswal, S. (2007) Cell survival responses to environmental stresses via the Keap1-Nrf2-ARE pathway. *Annu. Rev. Pharmacol. Toxicol.* **47**, 89–116 [CrossRef Medline](#)
- Tamborero, D., Gonzalez-Perez, A., Perez-Llamas, C., Deu-Pons, J., Kandath, C., Reimand, J., Lawrence, M. S., Getz, G., Bader, G. D., Ding, L., and Lopez-Bigas, N. (2013) Comprehensive identification of mutational cancer driver genes across 12 tumor types. *Sci. Rep.* **3**, 2650 [CrossRef Medline](#)
- Hayes, J. D., and McMahon, M. (2006) The double-edged sword of Nrf2: subversion of redox homeostasis during the evolution of cancer. *Mol. Cell* **21**, 732–734 [CrossRef Medline](#)
- Padmanabhan, B., Tong, K. I., Ohta, T., Nakamura, Y., Scharlock, M., Ohtsui, M., Kang, M. I., Kobayashi, A., Yokoyama, S., and Yamamoto, M. (2006) Structural basis for defects of Keap1 activity provoked by its point mutations in lung cancer. *Mol. Cell* **21**, 689–700 [CrossRef Medline](#)
- Kensler, T. W., Egner, P. A., Agyeman, A. S., Visvanathan, K., Groopman, J. D., Chen, J. G., Chen, T. Y., Fahey, J. W., and Talalay, P. (2013) Keap1-nrf2 signaling: a target for cancer prevention by sulforaphane. *Top. Curr. Chem.* **329**, 163–177 [CrossRef Medline](#)
- Lan, A., Li, W., Liu, Y., Xiong, Z., Zhang, X., Zhou, S., Palko, O., Chen, H., Kapita, M., Prigge, J. R., Schmidt, E. E., Chen, X., Sun, Z., and Chen, X. L. (2016) Chemoprevention of oxidative stress-associated oral carcinogenesis by sulforaphane depends on NRF2 and the isothiocyanate moiety. *Oncotarget* **7**, 53502–53514 [Medline](#)
- Ma, Q., and He, X. (2012) Molecular basis of electrophilic and oxidative defense: promises and perils of Nrf2. *Pharmacol. Rev.* **64**, 1055–1081 [CrossRef Medline](#)
- Jaramillo, M. C., and Zhang, D. D. (2013) The emerging role of the Nrf2-Keap1 signaling pathway in cancer. *Genes Dev.* **27**, 2179–2191 [CrossRef Medline](#)
- Sporn, M. B., and Liby, K. T. (2012) NRF2 and cancer: the good, the bad and the importance of context. *Nat. Rev. Cancer* **12**, 564–571 [CrossRef Medline](#)
- Wang, H., Liu, X., Long, M., Huang, Y., Zhang, L., Zhang, R., Zheng, Y., Liao, X., Wang, Y., Liao, Q., Li, W., Tang, Z., Tong, Q., Wang, X., Fang, F., et al. (2016) NRF2 activation by antioxidant antidiabetic agents accelerates tumor metastasis. *Sci. Transl. Med.* **8**, 334ra351 [CrossRef Medline](#)
- Kitamura, H., and Motohashi, H. (2018) NRF2 addiction in cancer cells. *Cancer Sci.* **109**, 900–911 [CrossRef Medline](#)
- Yamamoto, M., Kensler, T. W., and Motohashi, H. (2018) The KEAP1-NRF2 system: a thiol-based sensor-effector apparatus for maintaining redox homeostasis. *Physiol. Rev.* **98**, 1169–1203 [CrossRef Medline](#)
- Zhu, J., Wang, H., Chen, F., Fu, J., Xu, Y., Hou, Y., Kou, H. H., Zhai, C., Nelson, M. B., Zhang, Q., Andersen, M. E., and Pi, J. (2016) An overview of chemical inhibitors of the Nrf2-ARE signaling pathway and their potential applications in cancer therapy. *Free Radic. Biol. Med.* **99**, 544–556 [CrossRef Medline](#)
- Wakabayashi, N., Itoh, K., Wakabayashi, J., Motohashi, H., Noda, S., Takahashi, S., Imakado, S., Kotsuji, T., Otsuka, F., Roop, D. R., Harada, T., Engel, J. D., and Yamamoto, M. (2003) Keap1-null mutation leads to postnatal lethality due to constitutive Nrf2 activation. *Nat. Genet.* **35**, 238–245 [CrossRef Medline](#)
- Camp, N. D., James, R. G., Dawson, D. W., Yan, F., Davison, J. M., Houck, S. A., Tang, X., Zheng, N., Major, M. B., and Moon, R. T. (2012) Wilms tumor gene on X chromosome (WTX) inhibits degradation of NRF2 protein through competitive binding to KEAP1 protein. *J. Biol. Chem.* **287**, 6539–6550 [CrossRef Medline](#)
- Chen, W., Sun, Z., Wang, X. J., Jiang, T., Huang, Z., Fang, D., and Zhang, D. D. (2009) Direct interaction between Nrf2 and p21(Cip1/WAF1) up-regulates the Nrf2-mediated antioxidant response. *Mol. Cell* **34**, 663–673 [CrossRef Medline](#)
- Hast, B. E., Goldfarb, D., Mulvaney, K. M., Hast, M. A., Siesser, P. F., Yan, F., Hayes, D. N., and Major, M. B. (2013) Proteomic analysis of ubiquitin ligase KEAP1 reveals associated proteins that inhibit NRF2 ubiquitination. *Cancer Res.* **73**, 2199–2210 [CrossRef Medline](#)
- Komatsu, M., Kurokawa, H., Waguri, S., Taguchi, K., Kobayashi, A., Ichimura, Y., Sou, Y. S., Ueno, I., Sakamoto, A., Tong, K. I., Kim, M., Nishito, Y., Iemura, S., Natsume, T., Ueno, T., Kominami, E., et al. (2010) The selective autophagy substrate p62 activates the stress responsive transcription factor Nrf2 through inactivation of Keap1. *Nat. Cell Biol.* **12**, 213–223 [CrossRef Medline](#)
- Lo, S. C., and Hannink, M. (2006) PGAM5, a Bcl-XL-interacting protein, is a novel substrate for the redox-regulated Keap1-dependent ubiquitin ligase complex. *J. Biol. Chem.* **281**, 37893–37903 [CrossRef Medline](#)
- Ma, J., Cai, H., Wu, T., Sobhian, B., Huo, Y., Alciivar, A., Mehta, M., Cheung, K. L., Ganesan, S., Kong, A. N., Zhang, D. D., and Xia, B. (2012) PALB2 interacts with KEAP1 to promote NRF2 nuclear accumulation and function. *Mol. Cell. Biol.* **32**, 1506–1517 [CrossRef Medline](#)
- Mulvaney, K. M., Matson, J. P., Siesser, P. F., Tamir, T. Y., Goldfarb, D., Jacobs, T. M., Cloer, E. W., Harrison, J. S., Vaziri, C., Cook, J. G., and Major, M. B. (2016) Identification and characterization of MCM3 as a Kelch-like ECH-associated protein 1 (KEAP1) substrate. *J. Biol. Chem.* **291**, 23719–23733 [CrossRef Medline](#)
- Wang, Q., Ma, J., Lu, Y., Zhang, S., Huang, J., Chen, J., Bei, J. X., Yang, K., Wu, G., Huang, K., Chen, J., and Xu, S. (2017) CDK20 interacts with KEAP1 to activate NRF2 and promotes radiochemoresistance in lung cancer cells. *Oncogene* **36**, 5321–5330 [CrossRef Medline](#)
- Suzuki, T., Seki, S., Hiramoto, K., Naganuma, E., Kobayashi, E. H., Yamaoka, A., Baird, L., Takahashi, N., Sato, H., and Yamamoto, M. (2017) Hyperactivation of Nrf2 in early tubular development induces nephrogenic diabetes insipidus. *Nat. Commun.* **8**, 14577 [CrossRef Medline](#)
- Chen, H., Hu, Y., Fang, Y., Djukic, Z., Yamamoto, M., Shaheen, N. J., Orlando, R. C., and Chen, X. (2014) Nrf2 deficiency impairs the barrier function of mouse oesophageal epithelium. *Gut* **63**, 711–719 [CrossRef Medline](#)
- Chorley, B. N., Campbell, M. R., Wang, X., Karaca, M., Sambandan, D., Bangura, F., Xue, P., Pi, J., Kleeberger, S. R., and Bell, D. A. (2012) Identification of novel NRF2-regulated genes by ChIP-seq: influence on retinoid X receptor α . *Nucleic Acids Res.* **40**, 7416–7429 [CrossRef Medline](#)
- Kobayashi, E. H., Suzuki, T., Funayama, R., Nagashima, T., Hayashi, M., Sekine, H., Tanaka, N., Moriguchi, T., Motohashi, H., Nakayama, K., and Yamamoto, M. (2016) Nrf2 suppresses macrophage inflammatory response by blocking proinflammatory cytokine transcription. *Nat. Commun.* **7**, 11624 [CrossRef Medline](#)
- Malhotra, D., Portales-Casamar, E., Singh, A., Srivastava, S., Arenillas, D., Happel, C., Shyr, C., Wakabayashi, N., Kensler, T. W., Wasserman, W. W., and Biswal, S. (2010) Global mapping of binding sites for Nrf2 identifies

- novel targets in cell survival response through ChIP-seq profiling and network analysis. *Nucleic Acids Res.* **38**, 5718–5734 [CrossRef Medline](#)
32. Hirotsu, Y., Katsuoka, F., Funayama, R., Nagashima, T., Nishida, Y., Nakayama, K., Engel, J. D., and Yamamoto, M. (2012) Nrf2-MafG heterodimers contribute globally to antioxidant and metabolic networks. *Nucleic Acids Res.* **40**, 10228–10239 [CrossRef Medline](#)
 33. Su, H., Hu, N., Yang, H. H., Wang, C., Takikita, M., Wang, Q. H., Giffen, C., Clifford, R., Hewitt, S. M., Shou, J. Z., Goldstein, A. M., Lee, M. P., and Taylor, P. R. (2011) Global gene expression profiling and validation in esophageal squamous cell carcinoma and its association with clinical phenotypes. *Clin. Cancer Res.* **17**, 2955–2966 [CrossRef Medline](#)
 34. Chen, H., Li, J., Li, H., Hu, Y., Tevebaugh, W., Yamamoto, M., Que, J., and Chen, X. (2012) Transcript profiling identifies dynamic gene expression patterns and an important role for Nrf2/Keap1 pathway in the developing mouse esophagus. *PLoS ONE* **7**, e36504 [CrossRef Medline](#)
 35. Chen, M., David, C. J., and Manley, J. L. (2012) Concentration-dependent control of pyruvate kinase M mutually exclusive splicing by hnRNP proteins. *Nat. Struct. Mol. Biol.* **19**, 346–354 [CrossRef Medline](#)
 36. Su, C. H., Hung, K. Y., Hung, S. C., and Tarn, W. Y. (2017) RBM4 regulates neuronal differentiation of mesenchymal stem cells by modulating alternative splicing of pyruvate kinase M. *Mol. Cell. Biol.* **37**, e00466–16 [CrossRef Medline](#)
 37. Gao, Y. B., Chen, Z. L., Li, J. G., Hu, X. D., Shi, X. J., Sun, Z. M., Zhang, F., Zhao, Z. R., Li, Z. T., Liu, Z. Y., Zhao, Y. D., Sun, J., Zhou, C. C., Yao, R., Wang, S. Y., et al. (2014) Genetic landscape of esophageal squamous cell carcinoma. *Nat. Genet.* **46**, 1097–1102 [CrossRef Medline](#)
 38. Lin, D. C., Hao, J. J., Nagata, Y., Xu, L., Shang, L., Meng, X., Sato, Y., Okuno, Y., Varela, A. M., Ding, L. W., Garg, M., Liu, L. Z., Yang, H., Yin, D., Shi, Z. Z., et al. (2014) Genomic and molecular characterization of esophageal squamous cell carcinoma. *Nat. Genet.* **46**, 467–473 [CrossRef Medline](#)
 39. Shibata, T., Kokubu, A., Saito, S., Narisawa-Saito, M., Sasaki, H., Aoyagi, K., Yoshimatsu, Y., Tachimori, Y., Kushima, R., Kiyono, T., and Yamamoto, M. (2011) NRF2 mutation confers malignant potential and resistance to chemoradiation therapy in advanced esophageal squamous cancer. *Neoplasia* **13**, 864–873 [CrossRef Medline](#)
 40. Zhang, D., Li, J., Wang, F., Hu, J., Wang, S., and Sun, Y. (2014) 2-Deoxy-D-glucose targeting of glucose metabolism in cancer cells as a potential therapy. *Cancer Lett.* **355**, 176–183 [CrossRef Medline](#)
 41. Chen, J., Xie, J., Jiang, Z., Wang, B., Wang, Y., and Hu, X. (2011) Shikonin and its analogs inhibit cancer cell glycolysis by targeting tumor pyruvate kinase-M2. *Oncogene* **30**, 4297–4306 [CrossRef Medline](#)
 42. Mitsuishi, Y., Taguchi, K., Kawatani, Y., Shibata, T., Nukiwa, T., Aburatani, H., Yamamoto, M., and Motohashi, H. (2012) Nrf2 redirects glucose and glutamine into anabolic pathways in metabolic reprogramming. *Cancer Cell* **22**, 66–79 [CrossRef Medline](#)
 43. Rolf, F., Huber, M., Kuehne, A., Kramer, S., Haertel, E., Muzumdar, S., Wagner, J., Tanner, Y., Böhm, F., Smola, S., Zamboni, N., Levesque, M. P., Dummer, R., Beer, H. D., Hohl, D., et al. (2015) Nrf2 activation promotes keratinocyte survival during early skin carcinogenesis via metabolic alterations. *Cancer Res.* **75**, 4817–4829 [CrossRef Medline](#)
 44. Saito, T., Ichimura, Y., Taguchi, K., Suzuki, T., Mizushima, T., Takagi, K., Hirose, Y., Nagahashi, M., Iso, T., Fukutomi, T., Ohishi, M., Endo, K., Uemura, T., Nishito, Y., Okuda, S., et al. (2016) p62/Sqstm1 promotes malignancy of HCV-positive hepatocellular carcinoma through Nrf2-dependent metabolic reprogramming. *Nat. Commun.* **7**, 12030 [CrossRef Medline](#)
 45. DeNicola, G. M., Chen, P. H., Mullarky, E., Sudderth, J. A., Hu, Z., Wu, D., Tang, H., Xie, Y., Asara, J. M., Huffman, K. E., Wistuba, I. I., Minna, J. D., DeBerardinis, R. J., and Cantley, L. C. (2015) NRF2 regulates serine biosynthesis in non-small cell lung cancer. *Nat. Genet.* **47**, 1475–1481 [CrossRef Medline](#)
 46. Ludtmann, M. H., Angelova, P. R., Zhang, Y., Abramov, A. Y., and Dinkova-Kostova, A. T. (2014) Nrf2 affects the efficiency of mitochondrial fatty acid oxidation. *Biochem. J.* **457**, 415–424 [CrossRef Medline](#)
 47. Uruno, A., Yagishita, Y., Katsuoka, F., Kitajima, Y., Nunomiya, A., Nagatomi, R., Pi, J., Biswal, S. S., and Yamamoto, M. (2016) Nrf2-mediated regulation of skeletal muscle glycogen metabolism. *Mol. Cell. Biol.* **36**, 1655–1672 [CrossRef Medline](#)
 48. Vander Heiden, M. G., and DeBerardinis, R. J. (2017) Understanding the intersections between metabolism and cancer biology. *Cell* **168**, 657–669 [CrossRef Medline](#)
 49. DeBerardinis, R. J., and Chandel, N. S. (2016) Fundamentals of cancer metabolism. *Sci. Adv.* **2**, e1600200 [CrossRef Medline](#)
 50. Holmström, K. M., Kostov, R. V., and Dinkova-Kostova, A. T. (2016) The multifaceted role of Nrf2 in mitochondrial function. *Curr. Opin. Toxicol.* **1**, 80–91 [CrossRef Medline](#)
 51. Sabouny, R., Fraunberger, E., Geoffrion, M., Ng, A. C., Baird, S. D., Screaton, R. A., Milne, R., McBride, H. M., and Shutt, T. E. (2017) The Keap1-Nrf2 stress response pathway promotes mitochondrial hyperfusion through degradation of the mitochondrial fission protein Drp1. *Antioxid. Redox Signal.* **27**, 1447–1459 [CrossRef Medline](#)
 52. Khan, A. U. H., Rathore, M. G., Allende-Vega, N., Vo, D. N., Belkhal, S., Orecchioni, S., Talarico, G., Bertolini, F., Cartron, G., Lecellier, C. H., and Villalba, M. (2016) Human leukemic cells performing oxidative phosphorylation (OXPHOS) generate an antioxidant response independently of reactive oxygen species (ROS) production. *EBioMedicine* **3**, 43–53 [CrossRef Medline](#)
 53. Krall, E. B., Wang, B., Munoz, D. M., Ilic, N., Raghavan, S., Niederst, M. J., Yu, K., Ruddy, D. A., Aguirre, A. J., Kim, J. W., Redig, A. J., Gainor, J. F., Williams, J. A., Asara, J. M., Doench, J. G., et al. (2017) KEAP1 loss modulates sensitivity to kinase targeted therapy in lung cancer. *eLife* **6**, e18970 [CrossRef Medline](#)
 54. Ramadori, P., Drescher, H., Erschfeld, S., Schumacher, F., Berger, C., Fragoulis, A., Schenkel, J., Kensler, T. W., Wruck, C. J., Trautwein, C., Kroy, D. C., and Streetz, K. L. (2016) Hepatocyte-specific Keap1 deletion reduces liver steatosis but not inflammation during non-alcoholic steatohepatitis development. *Free Radic. Biol. Med.* **91**, 114–126 [CrossRef Medline](#)
 55. Christofk, H. R., Vander Heiden, M. G., Harris, M. H., Ramanathan, A., Gerstzen, R. E., Wei, R., Fleming, M. D., Schreiber, S. L., and Cantley, L. C. (2008) The M2 splice isoform of pyruvate kinase is important for cancer metabolism and tumour growth. *Nature* **452**, 230–233 [CrossRef Medline](#)
 56. Dayton, T. L., Jacks, T., and Vander Heiden, M. G. (2016) PKM2, cancer metabolism, and the road ahead. *EMBO Rep.* **17**, 1721–1730 [CrossRef Medline](#)
 57. Wang, Y., Liu, J., Jin, X., Zhang, D., Li, D., Hao, F., Feng, Y., Gu, S., Meng, F., Tian, M., Zheng, Y., Xin, L., Zhang, X., Han, X., Aravind, L., and Wei, M. (2017) O-GlcNAcylation destabilizes the active tetrameric PKM2 to promote the Warburg effect. *Proc. Natl. Acad. Sci. U.S.A.* **114**, 13732–13737 [CrossRef Medline](#)
 58. Wang, Y. H., Israelsen, W. J., Lee, D., Yu, V. W. C., Jeanson, N. T., Clish, C. B., Cantley, L. C., Vander Heiden, M. G., and Scadden, D. T. (2014) Cell-state-specific metabolic dependency in hematopoiesis and leukemogenesis. *Cell* **158**, 1309–1323 [CrossRef Medline](#)
 59. Lunt, S. Y., Muralidhar, V., Hosios, A. M., Israelsen, W. J., Gui, D. Y., Newhouse, L., Ogrodzinski, M., Hecht, V., Xu, K., Acevedo, P. N., Hollern, D. P., Bellinger, G., Dayton, T. L., Christen, S., Elia, I., et al. (2015) Pyruvate kinase isoform expression alters nucleotide synthesis to impact cell proliferation. *Mol. Cell* **57**, 95–107 [CrossRef Medline](#)
 60. Israelsen, W. J., Dayton, T. L., Davidson, S. M., Fiske, B. P., Hosios, A. M., Bellinger, G., Li, J., Yu, Y., Sasaki, M., Horner, J. W., Burga, L. N., Xie, J., Jurczak, M. J., DePinho, R. A., Clish, C. B., et al. (2013) PKM2 isoform-specific deletion reveals a differential requirement for pyruvate kinase in tumor cells. *Cell* **155**, 397–409 [CrossRef Medline](#)
 61. Lau, A. N., Israelsen, W. J., Roper, J., Sinnamon, M. J., Georgeon, L., Dayton, T. L., Hillis, A. L., Yilmaz, O. H., Di Vizio, D., Hung, K. E., and Vander Heiden, M. G. (2017) PKM2 is not required for colon cancer initiated by APC loss. *Cancer Metab.* **5**, 10 [CrossRef Medline](#)
 62. Dayton, T. L., Gocheva, V., Miller, K. M., Bhutkar, A., Lewis, C. A., Bronson, R. T., Vander Heiden, M. G., and Jacks, T. (2018) Isoform-specific deletion of PKM2 constrains tumor initiation in a mouse model of soft tissue sarcoma. *Cancer Metab.* **6**, 6 [CrossRef Medline](#)
 63. Dayton, T. L., Gocheva, V., Miller, K. M., Israelsen, W. J., Bhutkar, A., Clish, C. B., Davidson, S. M., Luengo, A., Bronson, R. T., Jacks, T., and Vander Heiden, M. G. (2016) Germline loss of PKM2 promotes metabolic

Hyperactive *Nrf2* in the esophagus

- distress and hepatocellular carcinoma. *Genes Dev.* **30**, 1020–1033 [CrossRef Medline](#)
64. Cortés-Cros, M., Hemmerlin, C., Ferretti, S., Zhang, J., Gounarides, J. S., Yin, H., Müller, A., Haberkorn, A., Chene, P., Sellers, W. R., and Hofmann, F. (2013) M2 isoform of pyruvate kinase is dispensable for tumor maintenance and growth. *Proc. Natl. Acad. Sci. U.S.A.* **110**, 489–494 [CrossRef Medline](#)
65. Romero, R., Sayin, V. I., Davidson, S. M., Bauer, M. R., Singh, S. X., LeBoeuf, S. E., Karakousi, T. R., Ellis, D. C., Bhutkar, A., Sánchez-Rivera, F. J., Subbaraj, L., Martinez, B., Bronson, R. T., Prigge, J. R., Schmidt, E. E., et al. (2017) Keap1 loss promotes Kras-driven lung cancer and results in dependence on glutaminolysis. *Nat. Med.* **23**, 1362–1368 [Medline](#)
66. Sayin, V. I., LeBoeuf, S. E., Singh, S. X., Davidson, S. M., Biancur, D., Guzelhan, B. S., Alvarez, S. W., Wu, W. L., Karakousi, T. R., Zavitsanou, A. M., Ubrico, J., Muir, A., Karagiannis, D., Morris, P. J., Thomas, C. J., et al. (2017) Activation of the NRF2 antioxidant program generates an imbalance in central carbon metabolism in cancer. *eLife* **6**, e28083 [CrossRef Medline](#)
67. Mayers, J. R., and Vander Heiden, M. G. (2017) Nature and nurture: what determines tumor metabolic phenotypes? *Cancer Res.* **77**, 3131–3134 [CrossRef Medline](#)
68. Sano, S., Itami, S., Takeda, K., Tarutani, M., Yamaguchi, Y., Miura, H., Yoshikawa, K., Akira, S., and Takeda, J. (1999) Keratinocyte-specific ablation of Stat3 exhibits impaired skin remodeling, but does not affect skin morphogenesis. *EMBO J.* **18**, 4657–4668 [CrossRef Medline](#)
69. Ho Sui, S. J., Mortimer, J. R., Arenillas, D. J., Brumm, J., Walsh, C. J., Kennedy, B. P., and Wasserman, W. W. (2005) oPOSSUM: identification of over-represented transcription factor binding sites in co-expressed genes. *Nucleic Acids Res.* **33**, 3154–3164 [CrossRef Medline](#)
70. Kamburov, A., Pentchev, K., Galicka, H., Wierling, C., Lehrach, H., and Herwig, R. (2011) ConsensusPathDB: Toward a more complete picture of cell biology. *Nucleic Acids Res.* **39**, D712–D717 [CrossRef Medline](#)
71. Kamburov, A., Wierling, C., Lehrach, H., and Herwig, R. (2009) ConsensusPathDB—a database for integrating human functional interaction networks. *Nucleic Acids Res.* **37**, D623–D628 [CrossRef Medline](#)